Institutions of the Russian Academy of Sciences
Joint Institute for High Temperatures RAS
Institute of Problems of Chemical Physics RAS
Kabardino-Balkarian State University

Physics of Extreme States of Matter — 2009

Chernogolovka, 2009

Physics of Extreme States of Matter — 2009

Edited by academician Fortov V. E., Karamurzov B. S., Temrokov A. I., Efremov V. P., Khishchenko K. V., Sultanov V. G., Levashov P. R., Kanel G. I., Iosilevski I. L., Milyavskiy V. V., Mintsev V. B., Petrov O. F., Savintsev A. P., Shpatakovskaya G. V.

This compendium is devoted to investigations in the fields of physics of high energy density and thermophysics of extreme states of matter. Interaction of powerful ion and electron beams with matter, interaction of intense laser, x-ray and microwave radiation with matter, techniques of intense energy fluxes generation, diagnostics of ultrafast processes, physics of shock and detonation waves, different models and results of theoretical calculations of equations of state of matter at high pressure and temperature, low-temperature plasma physics, issues of physics and power engineering, and technology projects are considered. The majority of the works has been presented at the XXIV International Conference on Interaction of Intense Energy Fluxes with Matter (March 1–6, 2009, Elbrus, Kabardino-Balkaria, Russia). The edition is intended for specialists in physical and technical problems of power engineering.

The conference is sponsored by the Russian Academy of Sciences, the Russian Foundation for Basic Research (grant No. 09-02-06056), and the International Science and Technology Center.

ISBN 978-5-901675-89-2

POWER INTERACTION WITH MATTER

BAND STRUCTURES OF SIMPLE AND NOBLE METALS AND THEIR MATERIAL PROPERTIES IN A TWO-TEMPERATURE STATE WITH HOT ELECTRONS OVERHEATED ABOVE A COLD CRYSTAL LATTICE BY AN ULTRASHORT LASER PULSE

***Inogamov N.A.*[*1], *Ashitkov S.I.*[2], *Zhakhovskii V.V.*[2], *Petrov Yu.V.*[1], *Khokhlov V.A.*[1], *Ovchinnikov A.V.*[2], *Komarov P.S.*[2], *Agranat M.B.*[2], *Anisimov S.I.*[1], *Nishihara K.*[3]**

[1]*ITP RAS, Chernogolovka, Russia,* [2]*JIHT RAS, Moscow, Russia,* [3]*ILE, Osaka, Japan*

**nailinogamov@googlemail.com*

Physics of ultrashort laser pulse (UsLP) interaction with matter is important as it is a base of many technologies from microchip surface fabrication, production of nanopowders, or layer film deposition to biomedical applications, see, e.g., [1]. A UsLP transfers metalls into a two-temperature (2T) state with $T_e \gg T_i$, where T_e, T_i are electron and ion temperatures. Duration of 2T state is $\sim 1-10$ ps. This is a new and rather artificial state. Indeed, energy density E_e of the electron subsystem right away the absorption of the UsLP may exceed the cohesion energy of condensed matter. These conditions were not interesting for researchers before beginning of the study of fast ions moving through solids [2] or before an invention of the UsLP [3] because they are incompatible with keeping of matter in a condensed state. In the case of UsLP the condensed matter may remain in condensed state as result of fast conductive cooling from irradiated surface into bulk of a target.

Now the 2T state is a subject of many fundamental studies. They are significant because thermodynamic (e.g., electron pressure p_e) and kinetic (e.g., conductivity σ) data about the 2T state are necessary for the understanding of processes initiated by a UsLP and for corresponding calculations. Our paper is devoted to this subject. Chromium-forsterite (wavelength λ =1240 nm, pulse duration τ_L =100 fs) or titanium-sapphire (λ =800 nm, τ_L =40 fs) lasers are used in the experimental part of the paper. Very high speed (temporal resolution $\sim \sqrt{2}\tau_L \sim 10^{-13}$ s) experimental pump-probe technique used in our work allows to follow fast non-equilibrium evolution of the irradiated target. But obtained experimental data are indirect. They contain only optical information about a reflected probe light wave—a coefficient of light reflection R and a phase ψ of a reflected wave (let's mention that R, ψ are functions of time delay t_{delay} between the pump and the probe FsLPs). There is a long way from (R, ψ) to the 2T thermodynamic/kinetic properties through a dielectric permittivity ε calculated from optical data. Therefore a physical model together with 2T hydrodynamic and molecular dynamic simulations are necessary to connect (R, ψ) and the 2T properties. There are three recent models including 2T, hydrodynamics, and optics [4–6]. Other 2T models do not include or 2T hydrodynamics, or optics. The term "2T hydrodynamics" means that the electron pressure p_e is included in the equations in addition to the 2T thermal effects (α, κ_e, C_e- an energy exchange, a coefficient of electronic heat conduction, an electron heat capacity). The main components of our model ([5]) are: the two-temperature equation of state, the many-body interatomic potential, the electron-ion energy exchange, the electron thermal conductivity, and optical properties of solid, liquid, and two phase solid-liquid mixture. The collision frequencies are taken from the recent quantum-mechanical molecular dynamics works, e.g., [7].

Comparison of experimental optical responses of simple (aluminum, Al) and noble (gold, Au) metals to pump irradiation at the incident fluences ~ 1 J/cm^2 shows qualitative differences. Fast increase of electron temperature T_e during a short time slice of pump action τ_L causes small changes of ε in Al (though T_e is high) and large changes in Au at similar T_e as shown in Fig. 1. Our analysis links this variation in ε to two factors. (i) There is a difference in the band structures of Al $3s^2 3p^1$ and Au $5d^{10}6s^1$. (ii) There is a decrease of a degeneration degree and a sharp growth of a collision frequency ν as result of this. Consequence of the ν-growth for absorption of the probe photons are different for Al and Au as the collision mechanisms are different.

Let's discuss a band structure and the dependence $Z(T_e)$ of number of the conduction electrons Z on T_e. In Al number $Z = 3$ does't change at our incident $F_{inc} < 2$ J/cm^2 and absorbed $F_{abs} < 0.3$ J/cm^2 fluences and corresponding maximum temperatures $T_e < 5$ eV. In gold at room temperature (r.t.) there are $Z = 1$ conduction and 10 d-electrons. A gap $E_g \approx 2$ eV separates the upper edge of the d-band and the Fermi level at r.t. $Z(T_e)$ increases in Au with the increase of T_e as it is shown in Fig. 2. The maximum $Z \sim 2-3$ at our fluences. Fig. 2 presents calculation with a simlified band structure. The d-band is described as the square distribution of the density of state (DOS), while the overlapping s and p bands are presented as an extension of a common parabolic DOS. This approach slightly underestimates Z. Electron energy $E_e(\rho = 19.3\text{g/cc}, T_e)$ is 8 eV/atom at $T_e = 3.3$ eV and $Z = 2$. Gold remains condensed for the example with maximum heating $T_e = 3.3$ eV owing to the electron heat conduction into the bulk of target although cohesive energy of Au is 3.4 eV/atom.

It is important that the collision mechanism depends on the band structure. This differs electron collisions in Al and Au. Main contributions are $\nu_{ei} + \nu_{ee}^{intraband} + \nu_{ee}^{interband}$, where ν_{ei} is electron-phonon col-

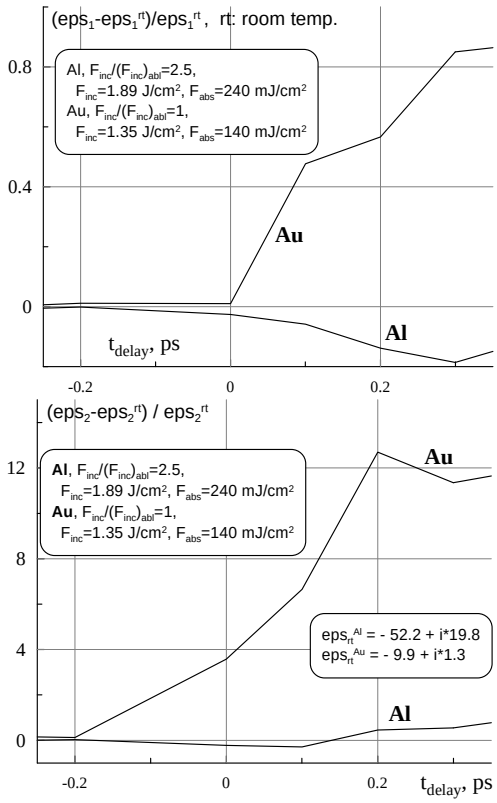

Figure 1. Qualitative difference (Al versus Au) in ability of the conduction electrons excited by the pump to absorb the probe photons. The difference is caused by the presence of the excited d-electrons in gold. To emphasize this the example with Al more hot than Au is shown. The ε is calculated by the Fresnel formula valid in the time range when the ε space profile maybe approximated by a step function.

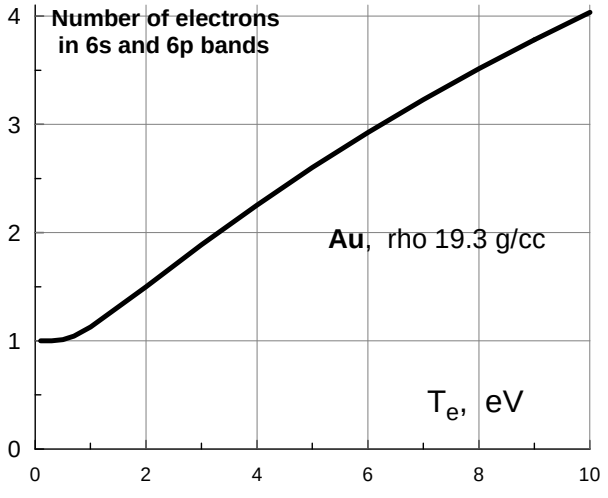

Figure 2. Increase of Z as result of thermal excitation of d-electrons into s,p bands.

lisions in a crystal or electron-ion collisions in a molten metal, $\nu_{ee}^{intraband} = b(E_F/\hbar)(T_e/T_F)^2$ is collisions between pairs of electrons both from the conductivity band ($E_F = k_B T_F$ is Fermi energy), $\nu_{ee}^{interband}$ is a frequency of collisions between electrons from different bands; they are absent in Al. In Au this results from the collisions between the s,p and d electrons. The ratio m_{eff}/m_e is ≈ 1 for the s,p electrons, while the d-band is narrow and the d-electrons are heavy $m_{eff} \gg m_e$.

It is supposed usually that ν_{ei} is a function of T_i only. This is true for Al with its simple band structure. The frequencies are: $\nu_{ei}^{solAl} = 4.5 \cdot 10^{11} T_i$ s^{-1}, $\nu_{ei}^{liqAl} = 1.1 \cdot 10^{14} T_i/(130 + 0.0367 T_i - 66700/T_i)$ s^{-1}, $\nu_{ei}^{solAu} = 1.2 \cdot 10^{11} T_i$ s^{-1}, $\nu_{ei}^{liqAu} = 2 \cdot 10^{14} + 2.3 \cdot 10^{11} T_i$ s^{-1} (the superscript "sol" means solid, "liq"—liquid). They are obtained from the one-temperature (1T) $T_e = T_i$ measurements. 2T simulations show that for the fluences given at Fig. 1 at $t_{delay} = 0.2$ ps temperatures of Al or Au are $T_i^{Al} = 1.3$ kK, $T_i^{Au} = 1$ kK (near the beginning of melting). At these T_i frequencies are $\bar{\nu}_{ei}^{solAl} \approx 0.15$, $\bar{\nu}_{ei}^{solAu} \approx 0.04$, where the normalized frequency is $\bar{\nu} = \nu/\omega_{probe}$, $\hbar\omega_{probe} = 2$ eV is the second harmonic of the chromium-forsterite laser. Melting $\nu_{ei}^{sol}|_{Tm} \to \nu_{ei}^{liq}|_{Tm}$ increases ν_{ei} 2.5 times in Al and 3 times in Au. At these short times metals are isochoricaly heated, pressure inside the heated surface layer is high, and melting temperatures T_m are higher than the low pressure values of T_m : $T_m = 933$ K (triple point, Al), the intersections of the solidus and the liquidus with the isohore $\rho = 2.71$ g/cc are 1.2 kK and 1.5 kK for Al, and 1337 K, 1.9 kK, and 2.05 kK for Au. We see that $\bar{\nu}_{ei}$ increases as the result of the lattice heating (the growth of T_i) even during short delay time. But the values $\bar{\nu}_{ei}$ remain significantly below the value $\bar{\nu}_{ei} \approx 1$ necessary to explain the changes of ε^{Au} in Fig. 1.

It is plausible that for Au with its overlapped d and s bands [8] there are another channels to enhance ν_{ei} as a result of increase of T_e to several eV. The growth of the number of conduction electrons $Z(T_e)$ illustrated in Fig. 2 increases the light absorption. The growth of the charge of ion Z magnifies the Coulomb cross-section of ions. As was shown this influences the elastic constants and melting temperature of Au [8]. This means that the effect is significant and may influence the values of ν_{ei} and α. The growth of Z increases the plasma frequency ω_{pl}. A new interesting channel of absorption is connected with d→i collisions when $Z-1$ holes in d-band interact and are scattered by ions. The holes absorb the probe photons and participate in the transfer of thermal energy from the conduction electrons to the cold lattice. The last process increases the e-i energy exchange coefficient α.

In case of Au our calculations show that α and ν_{ei} are related by the following equation $\nu_{ei}^{sol} = \alpha^{sol}(T_e)/nk_B](T_i/\theta)(T_F/\theta)$, where α is an e-i energy exchange, θ is Debye temperature. Similar relation should exists in a melt. It is proposed that in Au the coefficient α is a significant function of T_e [9–11] ten times increasing in the range $T_e = 3 - 20$ kK and after that saturating. If this is the case the frequency ν_{ei} will increase proportionally.

Let's analyze a role of the e-e collisions. In Al only $\nu_{ee}^{intraband}$ is possible. In Au an additional hypothetic channel of light absorption through $\nu_{ee}^{interband}$ may be significant. This frequency may be of order of the electron atomic frequency when T_e is high and $Z-1$ is ~ 1, see Fig. 2. This may explain results shown in Fig. 1.

The T_e enhancement of ν_{ei} and $\nu_{ee}^{intraband}$ presents two new mechanisms of absorption. The quantitative estimate of them should be developed in future. The sole term included in the physical models so far [4, 6] is $\nu_{ee}^{intraband}$. Below we will refer to it as simply ν_{ee}. The term ν_{ee} can ensure an immediate growth of absorption as T_e increases. At $T_e \sim T_F$ the electron-electron collision frequency ν_{ee} should be of order of atomic frequency, and $\bar{\nu}_{ee} > 1$. Why then the changes in ε_{Al} in Fig. 1 are small?

We have to split the frequency $\nu_{ee} = b(E_F/\hbar)(T_e/T_F)^2$, $b \sim 1$, into two different frequencies: one for diffusion, while the other for light absorption. They are $\nu_{ee} = b(E_F/\hbar)(T_e/T_F)^2$ (heat conductivity) and $\nu_{ee}^{Umkl} = \xi b(E_F/\hbar)(T_e/T_F)^2$ (electrical resistivity or photon absorption), $\xi < 1$. The "weight" coefficient ξ may differ from zero only as result of the Umklapp effect. The Umklapp processes operate if crystal lattice exists. But experiment shows that the changes in ε_{Al} are small. This means that $\xi \ll 1$. Why? A possible explanation is: in spite of the lattice existence at the short time delays the space-periodic correlations in the electron Bloch functions are broken as result of high e-e collisions frequency.

Evolution of the reflectivity $R(t)$ normalized to $R_o = R(-\infty)$ is shown in Fig. 3, where R_o is the reflectivity of surface before the pump action. The pump is p-polarized, angle of incidence is 45^o, and $\lambda_{pump} = 1240$ nm, the probe comes at the normal incidence relative to the frontal plane of the target. The crosses in Fig. 3 mark results of the pump-probe measurements. The theoretical curves (1, 2, 3) correspond to two Umklapp weights and two approximations of the parallel band (PB) absorption. The effective mass in Al is varied in the range $m_{eff} = (1.2 - 1.7)m_e$. The ε is presented as a sum [12–15] of the Drude $\varepsilon_{Dr} = 1 - [\omega_{pl}^2/(\omega^2 + \nu^2)](1 - i\nu/\omega)$ and the parallel bands D_{bb} terms

$$\varepsilon = \varepsilon_{Dr}(\omega, \nu, Z/m_{eff}) + D_{bb}(\nu), \qquad (1)$$

where $\nu = \nu_{ei} + \nu_{ee}^{Umkl}$. The PB interband addition D_{bb} in (1) is important in solid Al at our light frequency ω_{probe} (the wavelength is $\lambda_{probe} = 620$ nm) and it disappears at high collision frequencies ν and in molten Al [5, 12–15]. Two analytical expressions denoted D_{bb}^{AS} and D_{bb}^{620} are used for approximation of the term D_{bb}. The cumbersome expression D_{bb}^{AS} is taken from [15]. We also use simple phenomenological expression $D_{bb}^{620} = (\varepsilon^{rt} - \varepsilon_{Dr}^{rt})/[1 + A(\bar{\nu}^2 - (\bar{\nu}^{rt})^2)]$, $A = 7-10$ for our value of the wavelength $\lambda_{probe} = 620$ nm. The superscript "rt" means room temperatute. D_{bb}^{620} decays at $\nu \to \omega_{probe}$ and gives *exact* value for ε at rt, while D_{bb}^{AS} presents the dependence on the variation of ω but has an appreciable error at the particular value of ω. This error influences results even at later t_{delay} when Al melts and D_{bb} disappears because in our experiments the reflectivity R and the phase ψ are measured relative to their rt values (R_o, ψ_o) : $R \to R/R_o$, $\psi \to \Delta\psi = \psi - \psi_o$.

Figs. 3 demonstrate that in the model the Umklapp weight ξ should be taken small to correspond to the measurements. This conclusion follows from the absence of the absorption well connected with the e-e collisions in the observations.

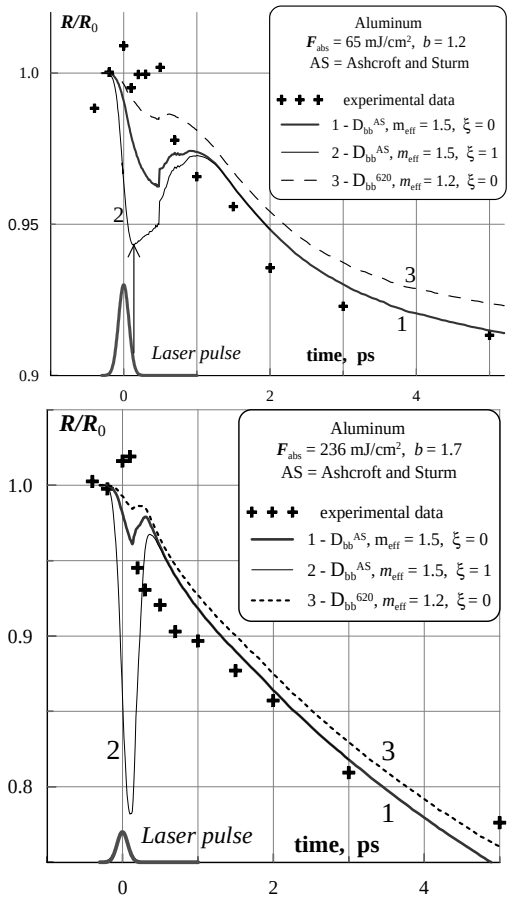

Figure 3. Absence of the "well" connected with ν_{ee} in the experimental absorptance history $R(t_{delay})$ (the crosses) of the Al target irradiated by the pump UsLP. Duration τ_L of the pump and the probe UsLP is 100 fs. The pump is shown as the Gaussian curve "Laser pulse".

The last conclusion is based on the measurements done at moderate intensities/fluences when an electron quivering energy is ~ 1 eV. The recent observations bring new discovery – formation of the well at high intensities. This is shown in Fig. 4. We see very

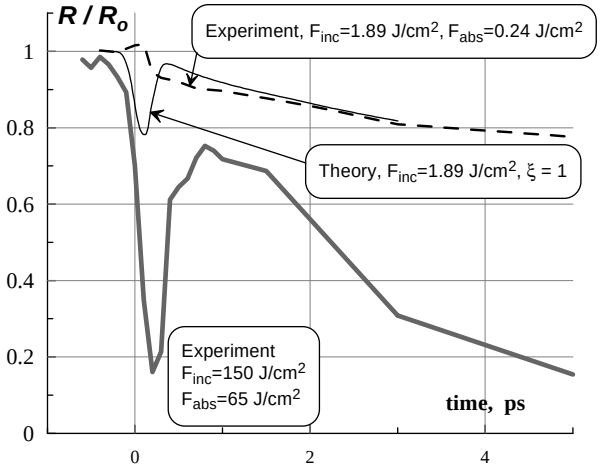

Figure 4. Appearance of the absorption well at very high intensities $I = 1.5 \cdot 10^{15}$ W/cm^2, Al.

fast huge decrease of the reflectivity followed with remarkable *fast recovery* – both obviously at an electronic time scale. After that much more slow decrease of $R(t)$ takes place at an ion time scale. The dashed and thin continuous curves are taken from the previous Figure to illustrate significance of magnification of the absorbed energy. The high I well resembles the theoretical e-e well at the moderate I. At the moment we do not have a simulation for the high I case. The reasons for formation of the high I well are unknown. The Umklapp is unlikely since the crystal periodicity and the Bloch functions seem unsignificant at high electron energies. If there is an another channel of a photon absorption in the electronic collisions then how to explain the fast recovery in Fig. 4? How to suppress these frequent collisions quickly? May be this is the optical manifestation of the Coulomb explosion of thin surface layer? The phase history of the high F case is given in Fig. 5 as the curve abcd.

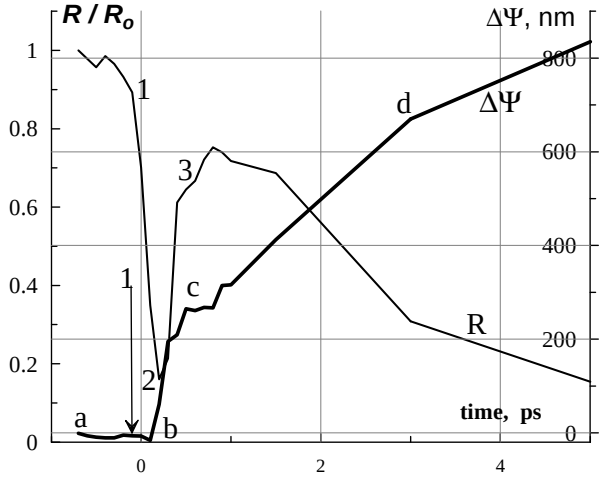

Figure 5. Short superfast expansion between the points b–c at the curve abcd $\Delta\psi(t)$ correlated with the well in $R(t)$. The high I dependence $R(t)$ is taken from the previous Figure.

If we suppose that the variation of the phase $\Delta\psi$ results from the shift of the reflecting surface (the surface of electron critical density n_c) then the velocity of the surface is 1060 km/s between the points b and c. Velocities between the points c–d and after the point d are: 180 km/s and 80 km/s, respectively. This velocity decay corresponds to the space dispersion of the first portion of the superfast ions. Dispersion means that the critical surface moves relative to the Lagrangian coordinate. The edge of the plasma cloud is hot, highly ionized, and the decrease in time of the electron density at any fixed value of the Lagrangian coordinate results from the coordinate dependent difference in the mass velocity – recombination at the early stages may be neglected. Let us mention that at moderate fluences $F_{inc} \sim 1$ J/cm^2 when initial velocities (velocities at the stage of the e-i relaxation when T_e and T_i equilibrates) are ~ 1 km/s the mechanism of the retardation of the cririca surface is qualitatively different. It is connected with the tensile strength of condensed phase.

This picture with rapid expansion of the small amount of the superfast ions uncovering underlying more cold ions can explain the recovery of R from the minimum point 2 to the point 3 in Figs. 4,5. But still the question remains why the recovery is so quick. Let's mention the fine effect with delayed sharp acceleration in the point b at the $\Delta\psi$ curve relative to the beginning of the sharp R drop marked as the point 1 at the R curve and the arrow 1 at the $\Delta\psi$ curve in Fig. 5. The time delay between the points 1 and b is 200 fs. Minimum of R in the point 2 is in the middle of the fast part b–c of the $\Delta\psi$ dependence. It is interesting that rather large values of $\Delta\psi \sim -15$ nm correspond to the precursor range a–b before the maximum of the pump at $t = 0$.

The pump-probe experiments at high I (similar to Figs. 4,5) are important as they open the way to generation of very high pressures in condensed media. Estimates based on $F_{abs} \sim \rho dv^2/2$, duration $t = d/v$, and the recoil momentum $pt = \rho dv$ gives $v \sim 120\sqrt{F_{65}/d_{30}}$ km/s, $t \sim 250 d_{30}^{3/2}/F_{65}^{1/2}$ fs, and $p \sim 0.5 F_{65}/d_{30}$ Gbar, where $F_{65} = F_{abs}/(65\text{J/cm}^2)$, $d_{30} = d/30\text{nm}$. p from this crude estimate is ~ 10 higher than in [16]. In contrast to the weakly decaying (due to dispersion of c_s) elastic shocks produced at moderate fluences (Figs. 1,3) the powerful shocks decay much faster as result of low energy penetration into bulk, strong dispersion (short impact) and energy loses for heating and ionization.

Let us return to the moderate I. The conclusion about the small weight ξ of the Umklapp absorption follows from the absence of the narrow e-e well in Fig. 3. This well is absent also in the data presented in [17]. The last data correspond to the range $0.2 - 1$ J/cm^2 of the s-polarized incident pump fluence.

There are four physical time scales: (i) $\tau_L \sim 0.1$ ps since the e-e relaxation is shorter than τ_L; (ii) the duration of the e-i thermal relaxation t_{eq}, when T_e and T_i equilibrate ($t_{eq} \sim 2 - 3$ ps for Al and $\sim 15 - 30$ ps for Au at our moderate fluences); (iii) the acoustic time $t_s = d_T/c_s$. Near the ablation threshold F_{abl} the maximum stretching is achieved at $t_{max} \sim t_s$ and nucleation in melt begins at $t_{nucl} \sim t_s$ [1, 18, 19]; for Al (Au) the time t_s and the heat penetration depth d_T are $\sim 15(100)$ ps, $\approx 100(200)$ nm. Significantly above F_{abl} the times t_{max} and t_{nucl} are shorter than t_s; (iv) the resolidification time is ~ 1 ns [20]. Above we consider the scale (i). Now let us consider the next scale. Evolution of the phase $\Delta\psi(t)$ measured by the pump-probe microinterferometric technique is shown in Fig. 6. Comparisons of the critical surface n_c trajectory $x_{nc}(t)$ and the phase $\Delta\psi(t)$ are presented in Fig. 7. The phase $\Delta\psi$ is a sum of the shifts $\Delta\psi_{nc}$ (the kinematical displacement) and $\Delta\psi_{phys}$ (the change in the physical state which causes the change of ε). These shifts are marked by the arrows a→b (forward) and b→c (backward) in Fig. 7.

In Al our analysis shows that the shift $\Delta\psi_{phys}$ is connected with melting of the crystal in the skin depth near surface. In Au the 2T simulation with $\nu_{ei} \propto \alpha$ and α taken from [9, 11] gives too small values for the relaxation time t_{eq} ($t_{eq} \sim C_i/\alpha$) and for the thermal depth d_T, $d_T \sim \sqrt{\chi t_{eq}} \sim \sqrt{(v_F^2/\nu)(C_i/\alpha)} \propto 1/\alpha$ if

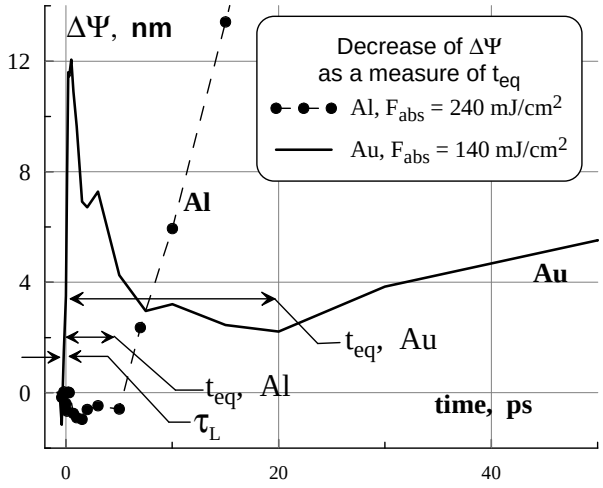

Figure 6. Two time scales τ_L and t_{eq}. The equilibration in Au is more slow $t_{eq}^{Al} < t_{eq}^{Au}$.

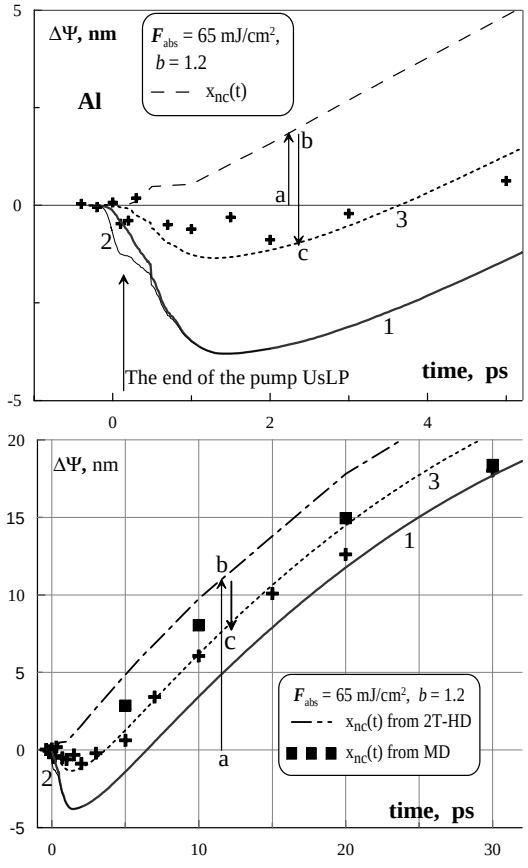

Figure 7. Delay of the growth of $\Delta\psi(t)$ in comparison with the shift $x_{nc}(t)$ as result of the change of ε during the e-i electron cooling and ion heating stage. The curves 1, 2, and 3 correspond to the same parameters as the curves 1, 2, 3 in Fig. 3. 2T-HD and MD refer to simulations done by the 2T hydrodynamics and molecular dynamics codes.

$\nu \sim \nu_{ei} \propto \alpha$, here $C_i = 3k_B n_i$ is the Dulong-Petit heat capacity, n_i is the ion concentration. This relaxation time is smaller than the time t_{eq} shown in Fig. 6. Therefore it seems that the coefficient α should be in between the low temperature ($T_e < 3$ kK) value $0.2 \cdot 10^{11}$ W/(cm^3 K) and the ten times larger value proposed in [9, 11]. Our 2T-HD and MD simulations together with experiments give the following parameters corresponding to the ablation threshold in Al(Au): $F_{abs} = 65(120)$ mJ/cm^2, the crater depth at the threshold is 50(100) nm, the maximum temperature at the instant of the equilibration is 2.2-2.5 kK. The work is supported by the RFBR grant No. 07-02-00764.

1. Inogamov N., Zhakhovskii V., Ashitkov S. I. *et al.* // JETP 2008. V. 107. P. 1.
2. Kaganov M. I., Lifshits I. M., Tanatarov L. V., // Sov. Phys.-JETP 1957. V. 4. P. 173.
3. Anisimov S., Kapeliovich B., Perel'man T. // Sov. Phys.-JETP 1974. V. 39. P. 375.
4. Agranat M. B., Andreev N. E., Ashitkov S. I. *et al.* // JETP Lett. 2007. V. 85. P. 271.
5. Inogamov N., Zhakhovskii V., Ashitkov S. *et al.* arXiv: 0812.2965 [physics.optics], 2008.
6. Colombier J., Combis P., Audouard E. *et al.* // Phys. Rev. E 2008. V. 77. P. 036409.
7. Recoules V. and Crocombette J. P. // Phys. Rev. B 2005. V. 72. P. 104202.
8. Recoules V., Clerouin J., Zerah G. *et al.* // Phys. Rev. Lett. 2006. V. 96. P. 055503.
9. Wang X. Y, Riffle R. M., Lee Y. S. *et al.* // Phys. Rev. B 1994. V. 50. P. 8016.
10. Chen J. K. and Beraun J. E. // J. Opt. A: Pure Appl. Opt. 2003. V. 5. P. 168.
11. Lin Z., Zhigilei L., and Celli V. // Phys. Rev. B 2008. V. 77. P. 075133.
12. Palik E. D. (ed.) Handbook Opt.Const.Solids. N.Y.: Academic Press, 1998.
13. Miller J. C. // Phil.Mag. 1969. V. 20. P. 1115.
14. Akashev L. A. and Kononenko V. I. // High Temperature 2001. V. 39(3). P. 384.
15. Ashcroft N. W., Sturm K. // Phys. Rev. B 1971. V. 3(6). P. 1898.
16. Eidmann K., Meyer-ter-Vehn J. *et al.* // Phys. Rev. E 2000. V. 62. P. 1202.
17. Kandyla N. W., Shih T., and Mazur E. // Phys. Rev. B 2007. V. 75. P. 214107.
18. Anisimov S. I., Inogamov N. A., Petrov Yu. V. *et al.* // Appl. Phys. A 2008. V. 92. P. 939.
19. Anisimov S. I., Inogamov N. A., Petrov Yu. V. *et al.* // Appl. Phys. A 2008. V. 92. P. 797.
20. Zhakhovskii V. V., Inogamov N. A., and Nishihara K. // JETP Lett. 2008. V. 87. P. 423.